Thermodynamic diesel engine cycle modeling and prediction of engine performance parameters

Mustafa Tuti[1*], Zehra Şahin[2] and Orhan Durgun[3]

mtuti@ktu.edu.tr

[1] *Faculty of Marine Science, Naval Architecture and Marine Eng. Dep., Karadeniz Technical University*
[2] *Faculty of Engineering, Mechanical Eng. Dep., Karadeniz Technical University*
[3] *Faculty of Engineering and Architecture, Mechanical Engineering Dep., Avrasya University*

Abstract

The aim of the present study is to develop a computer code for determining complete cycle, performance parameters and exhaust emissions of diesel engines. For this purpose, a computer program has been used and improved with new assumptions. To compute diesel engine cycle, zero-dimensional intake and exhaust model given by Durgun, zero-dimensional compression, combustion and expansion model given by Ferguson have been used and improved with new assumptions. Using the developed computer program, complete engine cycle, performance parameters and exhaust emissions can be determined easily. The values of the cylinder pressure and engine performance parameters predicted by the presented model matched closely with the other theoretical models and experimental data. Also, this program can be adapted and used practically for various parametric, alternative fuel and water addition studies in diesel engines.

Keywords: Diesel engine cycle, Engine performance characteristics, Simulation Models, Computer Code

1. Introduction

Modern diesel engine cycles can be predicted by applying a variety of simulation models. These models are used for optimization of engine parameters, investigation of control strategies or evaluation phenomena that are difficult to measure. In practice, using engine cycle simulation methods, the number of expensive experiments studies could be reduced and very useful results could be obtained for prediction of engine design parameters in a short time. Thus, these simulation models reduce the cost and time necessitate for engine development. New simulation models are constantly in development and the capabilities of currently available tools are being extended and continually improved. Also, these models are found to be prominent tools for arriving at the optimum designs (Pasternak and Mauss, 2009) & (Shrivastava et al., 2002) & (Bedford et al., 2000).

In the relevant literature, a number of modeling approaches (Pasternak and Mauss, 2009), (Ferguson, 1986) have been proposed and tested with various degrees of success. These models have been classified as phenomenological models and multi-dimensional models or fluid mechanics models (Sahin and Durgun, 2008).Phenomenological models are based on empirical relations to describe or quantify the individual processes that occur in an engine, such as: intake and exhaust, fuel-air mixing, ignition delay, combustion, heat transfer. Furthermore, phenomenological models can be further classified as; single zone, two zone, three zone, and multizone models (Pasternak and Mauss, 2009) , (Sahin and Durgun, 2008). Multidimensional models are based on numerical solution of the fundamental differential equations which govern the fluid motion and the combustion process (Bedford et al., 2000) & (Sindhu et al., 2014). The governing equations are developed and solved for the combustion chamber which is

divided into a fine geometric mesh. Although these models are capable of providing detailed information about both spatial and temporal resolution of the quantities of interest, they require large amounts of computer time and storage capacity (Bedford et al., 2000) & (Sindhu et al., 2014). Thus, if it is desired to examine the effects of all parameters on combustion and pollutant emissions more practical methods such as phenomenological models must be used (Sahin and Durgun, 2008) , (Kökkülünk et al., 2013). Many phenomenological (Sahin and Durgun, 2008), (Kökkülünk et al., 2013), (Qi et al., 2011) and multidimensional model (Tutak and Jamrozik, 2016), (Savioli, 2015) studies on diesel combustion, engine performance parameters and exhaust emission can be found in the literature. Tutak et al. (2016) developed a computational fluid dynamics (CFD) model of a turbocharged diesel engine (1CT107) powered by diesel fuel. In the simulation tests, they analyzed the effects of the ignition timing on the thermodynamic parameters and emissions of toxic components. They verified the model of the test engine and it was then used to optimize the thermodynamics cycle for the test engine. They found that the engine model was at acceptable accuracy and it was suitable for emissions modeling. Savioli (2015) developed a methodology to perform reliable CFD analysis for a 2-Stroke engine, with the support of a conventional steady flow test bench. This methodology is applied to a 2-Stroke engine prototype, for which a comprehensive set of experimental data is available. The achieved good agreement between simulation and experimental data shows the success of the proposed approach. Sahin and Durgun improved a multi-zone combustion model (phenomenological model) to predict the parameters of diesel engine cycles and performance. The values of the cylinder pressure and engine performance parameters predicted by this model matched closely with the other theoretical models and experimental data. Also, this program was adapted and used practically for various parametric and alternative fuel studies (Sahin and Durgun, 2008), (Sahin and Durgun, 2007a), (Sahin and Durgun, 2007b). Qi et al. (2011) proposed a quasi-dimensional combustion model of diesel engine which is based on a new simplified phase-divided spray mixing model. The comparisons with the other methods show that the relative error of effective power and break specific fuel consumption (BSFC) is less than 2.8 % and the relative error of nitric oxide and soot emissions is less than 9.1 % (Qi et al., 2011). Kökkülünk et al. (2013) investigated a thermodynamic simulation model for a steam injected diesel engine for determining of engine characteristics and NO emissions by using zero-dimensional single-zone combustion approximation. By comparing thermodynamic simulation model with experimental data, it can be seen that engine characteristics and NO emissions are closed to actual values at the levels of 1.5 % maximum error (Kökkülünk et al. 2013). Phenomenological and multidimensional modelings are often used to determine the complete engine cycle, engine performance characteristics and exhaust emissions for various engines as well as diesel engines. By this way, very useful results have been obtained for developing diesel engines. For this reason, these models have constantly been developed.

It can be seen from the above summarized relevant publications that many phenomenological and multidimensional model for diesel engines have been developed in the literature. However, further improvements of the complete cycle models for diesel engines is very important. For this purpose, in the present study, a computer code has been used and developed with new assumptions to assess complete cycle, performance parameters and exhaust emissions of diesel engines.

2. Description of the model

2.1. Thermodynamic simulation correlations

2.1.1. Calculation of compression, combustion and expansion strokes

In the present study, a computer program has been used for the prediction of diesel engine cycle and engine performance parameters. For calculation of DI diesel engine cycles, zero dimensional single-zone thermodynamic combustion model developed by Ferguson (1986) has been used and modified with new

assumptions. Here, a brief information about this model has been presented. In a diesel engine, the masses of burned fuel and air has been determined by using the following relations.

$$\frac{dm_a}{d\theta} = \frac{-m_l/\omega}{1 + \phi F_s}$$

(1)

$$\frac{dm_f}{d\theta} = \frac{1}{\omega}\left(-\frac{m_l \phi F_s}{1+\phi F_s}\right)$$

(2)

$$\frac{dm}{d\theta} = -\frac{\dot{m}_l}{\omega}$$

(3)

where ω is the angular speed, ϕ is the equivalence ratio, F_s is the stoichiometric fuel-air ratio. Eq. (1, 2) and the following energy equation (4) have been applied to the cylinder contents.

$$\frac{dU}{d\theta} = -\frac{\dot{Q}_l}{\omega} - P\frac{dV}{d\theta} - \frac{\dot{m}_l h_l}{\omega} + \frac{\dot{m}_f h_f}{\omega}$$

(4)

In eq. 4, the left hand side terms show heat transfer, work, blowby energy and energy provided by injected fuel, respectively. Some terms in this equation have been expressed as follows.

$$\dot{Q}_l = h\left(\frac{\pi b^2}{2} + \frac{4V}{b}\right)(T-T_w)$$

(5)

$$\frac{\dot{m}_{fi}}{m_{fi}} = \frac{\omega}{\theta_d \Gamma(n)}\left(\frac{\theta-\theta_s}{\theta_d}\right)^{n-1} \exp\left[\frac{-(\theta-\theta_s)}{\theta_d}\right]$$

(6)

$$\dot{m}_l = \frac{Cm}{\omega} = \frac{C(m_a+m_f)}{\omega}$$

(7)

where b is the cylinder bore, T_w is the cylinder wall temperature, θ, θ_s and θ_d are the crank angle, the start of the injection, the injection duration respectively, m_{fi} is the total mass of fuel to be injected per cycle, $\dot{m}_{fi}$ is the mass of injected fuel, c is the blowby coefficient, h is the heat transfer coefficient, V is the volume of cylinder and Γ is the gamma function and it has been determined approximately from the related asymototic formula.

$$\ln\Gamma(n) = \left(n_1 - \frac{1}{2}\right)\ln(n_1) - n_1 + \frac{1}{2}\ln(2\pi) + \frac{1}{12n_1} - \frac{1}{360n_1^3} + \frac{1}{1260n_1^5} - \frac{1}{1680n_1^7}$$

(8)

where n_1 is the injection parametre and it could be selected as $1 \le n_1 \le 2$ for open combustion chamber; $3 \le n_1 \le 5$ divided combustion chamber. This value is highly dependent upon the design parameters and the fuel properties. In the present study, n_1 is selected as 1.3 for common-rail direct injection diesel engine. By solving these ordinary differential equations (1), (2) and (4) simultaneously during compression,

combustion and expansion processes by using Runge-Kutta 5 method, V, m_a m_f and U can be calculated. Thus, by using these obtained U, V values and $U = mu(T,P,\phi)$, $V = mv(T,P,\phi)$, cylinder temperature and pressure have been calculated by using Newton-Raphson iteration. For determination of mean gas temperature and pressure values the following relations have been used.

$$T_{i+1} = T_i + \Delta T \tag{9}$$

$$p_{i+1} = p_i + \Delta p \tag{10}$$

$$\Delta T = \frac{-V \left[\dfrac{10\left(\dfrac{du}{d\theta}\right)}{p\dfrac{\partial \ln \upsilon}{\partial \ln p}} + \left(\dfrac{d\upsilon}{d\theta}\right)\left(\dfrac{\partial \ln \upsilon}{\partial \ln T} + \dfrac{\partial \ln \upsilon}{\partial \ln p}\right) \right]}{\dfrac{V^2}{T}\left[\left(-\dfrac{10 c_p T}{pV} + \dfrac{\partial \ln \upsilon}{\partial \ln T}\right)\left(-\dfrac{\partial \ln \upsilon}{\partial \ln p}\right) + \dfrac{\partial \ln \upsilon}{\partial \ln T}\left(\dfrac{\partial \ln \upsilon}{\partial \ln T} + \dfrac{\partial \ln \upsilon}{\partial \ln p}\right) \right]} \tag{11}$$

$$\Delta p = \frac{-\dfrac{pV}{T}\left[\dfrac{10 c_p T}{pV} - \dfrac{\partial \ln \upsilon}{\partial \ln T}\right]\dfrac{d\upsilon}{d\theta} - \dfrac{10\dfrac{du}{d\theta}\dfrac{\partial \ln \upsilon}{\partial \ln T}}{p}}{\dfrac{V^2}{T}\left[\left(-\dfrac{10 c_p T}{pV} + \dfrac{\partial \ln \upsilon}{\partial \ln T}\right)\left(-\dfrac{\partial \ln \upsilon}{\partial \ln p}\right) + \dfrac{\partial \ln \upsilon}{\partial \ln T}\left(\dfrac{\partial \ln \upsilon}{\partial \ln T} + \dfrac{\partial \ln \upsilon}{\partial \ln p}\right) \right]} \tag{12}$$

In relations (11) and (12), thermodynamic properties such as c_p, h etc. have been calculated step by step by using determined pressure and temperature. To compute these properties, combustion products have been determined by Olikara and Borman's method. Here, thermodynamic properties at low and high temperatures have been computed by using FARG and ECP subroutine, which is developed by Ferguson. After determination of combustion products, various thermodynamic properties have been determined. In order to solve the differential equations (1, 2 and 4) given above, the RATES subroutines developed by Ferguson (1986) have been modified and used. To solve temperature and pressure for U, V and f, STATE subroutines developed by Ferguson (1986).

2.1.2. Calculation of intake and exhaust strokes

Intake and exhaust processes are computed by using Durgun's (1991) method in which temperature and pressure at the end of the intake process have been calculated from properties of gas mixtures and Bernoulli equation, respectively, as follows:

$$T_a = \frac{(T_0 + \Delta T + \gamma_r T_r)}{1 + \gamma_r} \qquad \text{(natural aspirated diesel engine)} \tag{13a}$$

$$T_a = \frac{(T_c' + \Delta T + \gamma_r T_r)}{1 + \gamma_r} \qquad \text{(turbocharged diesel engine)} \tag{13b}$$

$$p_a = p_0 - \Delta p_a \qquad \text{(natural aspirated diesel engine)} \tag{14a}$$

$$p_a = p_c' - \Delta p_a \qquad \text{(turbocharged diesel engine)} \tag{14b}$$

$$\Delta p_a = \left(\beta^2 + \xi\right)\frac{V_m^2}{2}\left(\frac{n}{n_N}\right)^2 \rho_a$$

where $\left(\beta^2+\xi\right)$ is the total loss coefficient in the intake system, n and n_N are the actual engine speed and nominal engine speed, respectively, V_m is the maximum flow speed in the intake system, ρ_a is the density of air, γ_r is the coefficient of the residual gas, T_0, $T_c^{'}$ and T_r are the surrounding air, the compressor outlet air and residual gas temperatures respectively, and ΔT is the temperature variation of the intake charge flowing through intake channel, $p_c^{'}$ is the compressor outlet air pressure. In the presented study, residual gases which exist in the cylinder have been taken into account by using coefficient of residual gases in the intake process calculations because these gases have an important effect on the intake gas properties. In the presented study, exhaust temperature has been chosen approximately at the beginning of cycle calculations. Then, after cycle calculations are completed, chosen and calculated the exhaust temperatures compared. If the difference ratio between these values is higher than 3%, the final value has been taken as T_r and the cycle calculation is performed again. This calculation procedure has been repeated iteratively until the difference ratio between these values becomes smaller than 3%. Thus, complete cycle control have been performed. Exhaust temperature calculation and this comparison procedure is done by using the following relations:

$$T_r = \frac{T_b}{\sqrt[3]{\dfrac{p_b}{p_r}}} \qquad (15)$$

$$\left|\frac{T_r - T_1}{T_r}\right| \leq 3\% \qquad (16)$$

where T_r, p_r are the calculated exhaust temperature and pressure values, respectively, T_1 is the selected exhaust gas temperature at the beginning of intake process, T_b, p_b are temperature and pressure values, respectively, at the end of the expansion stroke.

2.1.3 Calculation of engine performance parameters

In the present study, correction factor of indicator diagram ϕ_i has been used to take into account the valve timing, injection advance and ignition delay effects. Thus, indicated work and indicated efficiency obtained from gross cycle simulation have been corrected as follows.

$$\eta_i = \frac{w_i(1+F_s\phi)}{F_s\phi(1-f)LHV}\varphi_i \qquad (17)$$

where η_i is indicated efficiency, w_i is indicated work per unit mass, f is residual mass fraction, LHV is lower heating value of the fuel.

After determining the complete diesel engine cycle, engine performance parameters such as effective power, effective efficiency, and specific fuel consumption are calculated from the relationships given by Heywood (1989) and Durgun (1991). In the presented study, effective engine characteristics have been computed by using the following mean effective pressure relationships given by Durgun (1991), while generally indicated engine performance have been given in the literature.

$$p_{m,m} = 10(a+bV_{p,m})\frac{p_c^{'}}{p_{mi}} \qquad \text{(turbocharged diesel engine)} \qquad (18)$$

$$p_{m,e} = p_{m,i} - p_{m,m} \tag{19}$$

For Renault K9K 700 type diesel engine, a and b values are selected as 0.089 and 0.0118, respectively. Eq.(18), $V_{p,m}$ is the mean piston speed and $p_{m,i}$ is the mean indicated pressure.

2.1.4. Calcutation of ignition delay

Ignition delay has been calculated by using Hardenberg and Hase (Sahin et al., 2014) correlation:

$$\theta_{id}(CA) = \left(0.36 + 0.22 Vpm\right) \exp\left[E_a \left(\frac{1}{RuT} - \frac{1}{17190} \right) \left(\frac{21.2}{\left(p - 12.4\right)} \right)^{0.63} \right] \tag{20}$$

where $V_{p,m}$ (m/sec) is mean piston speed, Ru (kJ/kmole/K) is universal gas constant, p (bar) is cylinder pressure, T (K) is cylinder temperature, E_a (kJkmole) is activation energy. The activation energy E_a is given by E_a = 618,840/(CN-25) where CN is the cetane number of the fuel. The average cetane number for the diesel fuel used for model engine tests is specified to be 45.

3. Accuracy control of the present model with applications for ndf

In the present study, the accuracy of the newly developed model has been controlled comparing with the experimental and theoretical data given in the relevant literature (Kökkülünk et al., 2013), (Qi et al., 2011), (Ottikkutti et al, 1991), (Kızıltan, 1988), (Sahin and Aksu, 2015). For this purpose, numerical results obtained from the presented model are compared with the experimental and the theoretical data of which are accepted to be at sufficient accuracy in the literature. In the comparisons with the experimental ones, Tuti's (2012), Kızıltan's (1988), Kökkülünk's (Kökkülünk et al., 2013) and Kunpeng's (Qi et al., 2011) experiments have been employed. Also, in the comparison with the relevant theoretical study, the results of Ottikkuti's model (Ottikkutti et al, 1991) has been used. The obtained computational results and comparisons have been presented as various tables and figures.

Here, firtsly the accuracy of the newly developed model has been controlled comparing with our experimental studies. These experiments were done in Mechanical Engineering Department KTU. In the experimental study, a turbocharged common-rail DI automotive diesel engine, Renault K9K 700 type, was used. The specifications of the test engine have been given in Table 1. Cylinder gas pressure was measured by using of an AVL GH12P type quartz pressure sensor without cooling (Sahin et al., 2014), (Tuti, 2012). Detailed information about pressure measurment can be found in refs. (Sahin et al., 2014), (Sahin and Aksu, 2015). The cylinder pressure values obtained from the present model have been compared to cylinder pressure values obtained from the experiments in Figs.1. As can be seen in Figs.1., the agreement between the predicted pressure values and the experimental results are generally good.

As shown in Fig.1.(a); the peak pressure for experiment at 2000 rpm is 156.34 bar and it occurs at 10° CA. On the other hand, the peak pressure value obtained from the present model is 157.23 bar and it occurs at 6° CA. It can be seen that the difference between these peak pressure values is 0.57%. The same results have been obtained for the other selected engine speeds. However, the maximum cylinder pressure values obtained from this model was found closely to the experimental results in the range of (0.57-4.5) % error rate at the selected engine speeds. It can be seen in Fig.1.(a) that the peak pressure

angles for predicted model is earlier than that of experiment at 2000 rpm. Possible reasons for this differences can be explained given as follows.

Some working parameters of engine such as ignition advanced (IA), etc. are not known. Actually, this engine has an electronic control unit (ECU). So, there is not constant IA for various engine speeds and diesel fuel injection has been controlled by for considering optimum operating conditions. In the pesent study, IA has been calculated aproximately by using determined experimentally heat release rate diagram (HRR) and relation (20). By using HRR, the crank angle at the the beginning of the combustion (θ_{comb}) has been determined. By taking into account starting point of combustion and relation (20), IA has approximately been computed ($\theta_{inj} = \theta_{comb} - \theta_{id}$).

Renault K9K700 type turbocharged diesel engine has common rail injection system and injectors of this system has five hole. In the present model, this feature of the injection system has not been considered. In the modeling study, it is assumed that the nozzle of the injector has one hole (that is, total injected diesel fuel has been used as input data for develop programme). It is well known that numbers and diameter of the holes of the nozzle are very important to form homogeneous air-fuel mixtures. This effect has not been taken into account in the present model. Also, pilot injection has been applied in the used engine. Here, this effect has not also be taken into account.
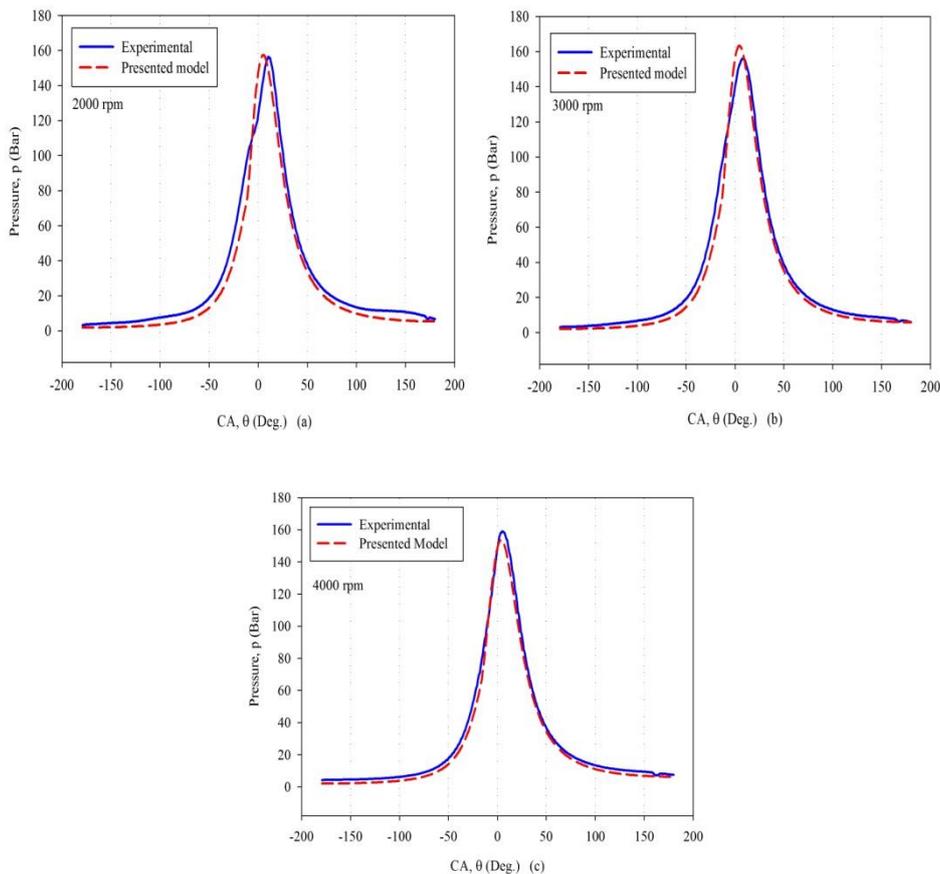
Figure 1. (a), (b) and (c) comparisons of cylinder pressure values obtained from the presented model with the experimental cylinder pressure data for 2000, 3000 and 4000 rpms.

In the present study, effective power and BSFC obtained from the present model have been compared with experimental results at (2000-4000) rpms in Figs.2. Effective power values obtained from the

present model and experiment are 29.13 kW and 31.96 kW respectively at the 2000 rpm. Hence, the difference between the effective powers is 8.8%. BSFC values obtained from present model and experiment are 0.2004 kg/kWh and 0.2205 kg/kWh, respectively at the 2000 rpm. Hence, the difference between these BSFC values is 9.1% at this engine speed. The differences between the present model and experimental data in terms of effective power and BSFC have shown the same variations for the other selected engine speeds. The effective power and BSFC obtained from modelling have approached to experimental data at the range of (0.3-8.8) % and (1.7-9.1) % error rate, respectively at the seleced engine speeds. The reasons for these differences have been given above paragraph. Besides these, the mechanical efficieny of the test engine is also unknown and this has been computed by using the relation (18).

Table 1. Main specifications of the engines used for comparisons of theoretical results with experimental data (n_n is nozzle holes number) [6, 7, 16, 19, 20]

	ε	D(mm)	H(mm)	p_p(bar)	θ_s(°)	d_n(mm)	Z	n_n
Renault K9K	18.25	76	80.5	up to 2000	change	0.12	4	5
Kızıltan	18-24	90	120	90-250	-22	0.36	1	1
Kökkülünk	17	108	100	175	-	-	1	-
Kunpeng	17	135	150	110	-10	0.36	1	4
Ottikkutti	16.8	106.5	127	120-490	-15	0.3	4	4
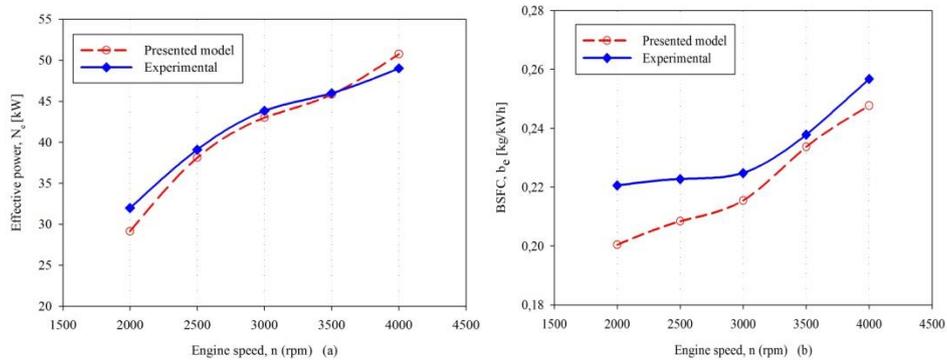
Figure 2. (a) and (b) Comparisons of effective power and BSFC values obtained from the presented model with experimental data

The other comparison has been performed by using Kızıltan's [19] experimental data. In Kızıltan's tests, a single cylinder, four-stroke, water cooled, variable compression ratio experimental engine manufactured by Tecquipment has been used. Main specifications of this test engine are given in Table 1. Comparisons of effective power and BSFC obtained from the presented model and Kızıltan's [19] experimental data have been shown in Figs.3 (a) and (b). As can be seen from these figures, the predicted results agree reasonably with the measured values. At 1300 rpm, the effective power computed by using the developed model for Kızıltan's engine has been obtained as 6.12 kW and the effective power given by Kızıltan was 5.615 kW. Thus, it can be seen that the difference between effective powers is 8.9 % at 1300 rpm. Also, BSFC values obtained from present model and experiment are 0.2647 kg/kWh and 0.281 kg/kWh respectively at the 1300 rpm. Hence, the difference between these BSFC values is 5.77%. For

different speeds, the maximum error rate between effective power and BSFC was found to be approximately 11%. This could be attributed to not knowning some parameters of the engine and selecting these parameters approximately and using an insufficient relation of mechanical losses and mechanical efficieny originally given for multi cylinder vehicle engine. This relation may not be suitable for the used engine. Similar error rates were observed in Şahin's multi-zone thermodynamic model for Kızıltan's experimental results (Sahin and Durgun, 2008).

In another comparison, experimental results given by Kökkülünk et al. have been used. Kökkülünk et al. were used a single cylinder, four-stroke, DI diesel engine in their experimental study (Kökkülünk et al., 2013). Table 1. shows the specifications of this engine. Fig.4 shows the comparison of cylinder pressure values obtained from the presented model with that of Kökkülünk's experimental data at 2200 rpm. As shown in Fig.4, the peak pressure for Kökkülünk's experiment at 2200 rpm is 68.13 bar and it occurs at 4° CA. On the other hand, the peak pressure value obtained from the present model is 67.74 bar and it occurs at 6° CA. It can be seen that the difference between these peak pressure values is 0.57 at this engine speed. Thus, a satisfactory conformity can be observed in Fig.4.
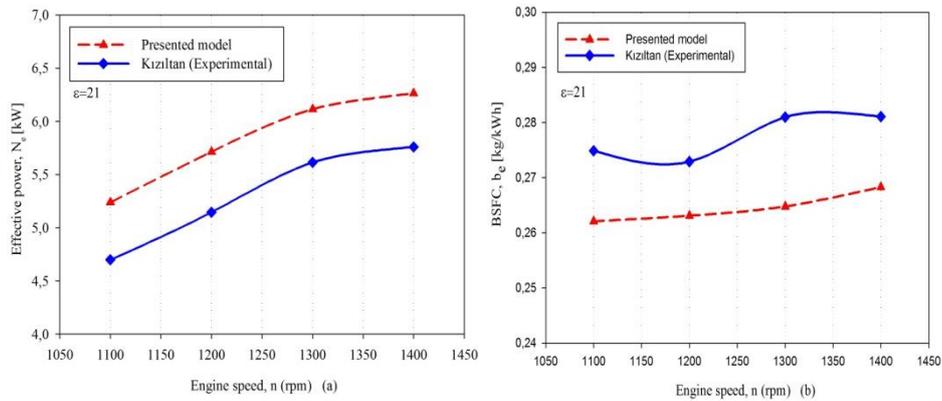
Figure 3. (a) and (b) Comparison of effective power and BSFC values obtained from the presented model and Kızıltan's experimental data
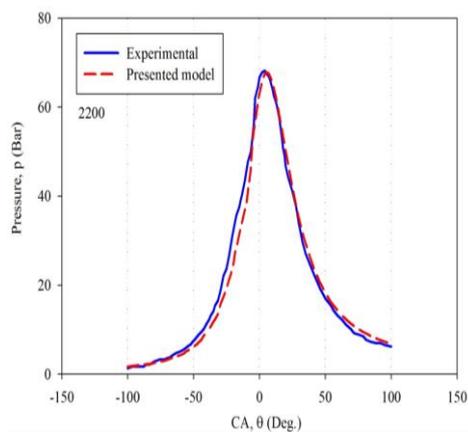
Figure 4. Comparisons of cylinder pressure values obtained from the presented model with the Kökkülünk's experimental data as a function of crank angle

Furthermore, effective power and BSFC obtained from the present model have been compared with Kökkülünk's data at (1700-2300) rpms in Figs.5. Effective power values obtained from the present model and experiment are 11.57 kW and 12.13 kW respectively at the 2000 rpm. Hence, the difference between these effective power values is 4.64%. The difference between the present model results and the

experimental data in terms of effective power shows the same variation for all selected engine speeds. BSFC values obtained from present model and experiment are 0.2672 kg/kWh and 0.2827 kg/kWh respectively at the 2000 rpm. Hence, the difference between these BSFC values is 5.48%. The difference ratios of BSFC according to the engine speeds obtained from the presented model were at levels of (3-11) % error. It can be seen In Fig. 5(a) that, difference between BSFC values obtained from the presented model and Kökkülünk's experimental data increase while engine speeds are increasing. This can be attributed to being used an empirical mean pressure of the mechanical losses relation originally developed for vehicle diesel engines as stated above. This equation may not be suitable for the used Kökkülünk's test engine.
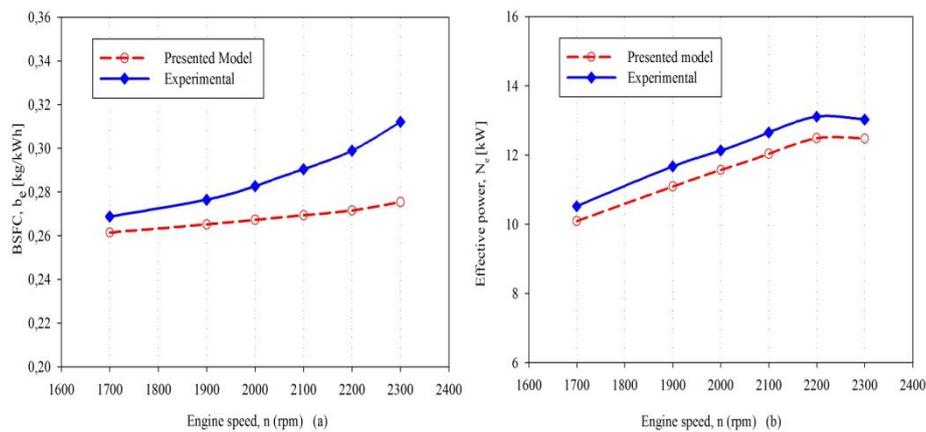
Figure 5. (a) and (b)Comparison of BSFC and effective power values obtained from the presented model and Kökkülünk's experimental data

Also, accuracy control of the present model have been performed by using Kunpeng's experimental data (Qi et al., 2011). In the Kunpeng's experimental study, a single cylinder, four-stroke, and water cooled, 1135 naturally aspirated diesel engine were used. Main specifications of this test engine are given in Table 1. In Fig.6 cylinder pressure values obtained from present model have been compared with Kunpeng's experimental data for 1500 rpm. As shown in Fig.6, at 1500 rpm, the peak pressure of Kunpeng's is 69.6 bar and it occurs at 13°CA, while in the presented model peak pressure is 70.8 bar and it occurs at 6°CA. Also, at 1500 rpm, the effective power and BSFC computed from the presented model are 13.496 kW and 256 g/kWh respectively. The effective power and BSFC values given by Kunpeng's experimental results are 14.7 kW and 245 g/kWh respectively. Thus, it can be seen that the difference effective power and BSFC values are 8.2 % and 4.5 % respectively. This could be attributed to not knowning some parameters of Kunpeng's test engine and selecting approximately these parameters. Injection pressure and IA have also been selected approximately and these parameters affects cylinder presure values. Also, injection strategy of the Kunpeng's test engine is not completely comply with gamma function used in present model ore injection parameter n_1 of this function may not be chosen well.

In the comparison with the relevant theoretical study, the results of Ottikkuti's model has also been used (Ottikkutti et al., 1991). The numerical results obtained from the presented model are compared with the theoretical results of Ottikkuti. In this theoretical study, Ottikkuti was used a 4 cylinder, four-stroke and turbocharged diesel engine. Main specifications of this test engine are given in Table 1. Effective power, the mean indicated pressure ($p_{m,i}$) and indicated thermal efficiency (η_i) values obtained from the

present model are compared with that of Ottikkutti's model. Effective power values obtained from the present model and Ottikkutti's model are 56.6 kW and 54.24 kW respectively at the 1500 rpm. Hence, the difference between these effective power values is 4.16 %. $p_{m,i}$ values obtained from the present model and Ottikkutti's model are 10.46 bar and 11.22 bar respectively at the 1500 rpm. Hence, the difference between these $p_{m,i}$ values is 7.27 %. η_i values attained from the present model and Ottikkutti's model are 0.459 and 0.497 respectively at this engine speed. These parameters show similar differences for 2100 rpm. Generally, effective power, $p_{m,i}$ and η_i values obtained from the present model showed maximum differences at the level of 9 % with Ottikkutti's model.
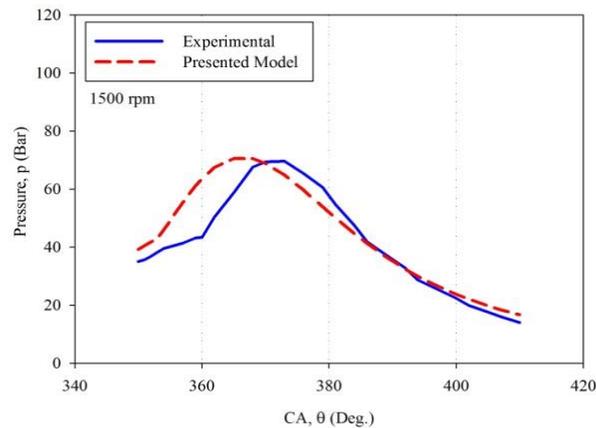
Figure 6. Comparisons of cylinder pressure values obtained from the presented model with Kunpeng's experimental cylinder pressure data as a function of crank angle

4. Conclusions

Results obtained from the development and verification studies and various applications of the presented diesel engine cycle model can be briefly summarized as follows:

1. The present model is able to predict the diesel engine cycles for neat diesel fuel. The model can predict the cylinder pressure and engine characteristics in good agreement with experimental and theoretical results and it can be applied easily and the run time is sufficiently low. Thus, it can be used effectively in various engine development and parametric studies.

2. Engine performance parameters and cylinder pressure values for only neat diesel fuel has been examined using present model. Actually, in the next studies we aimed to investigate the effect of addition of water to the intake air manifold in diesel engines by using this cycle model. Thus, this model will be adapted to addition of water to the intake air manifold of diesel engine in the near future. The theoretical studies on water addition have been started.

References

Bedford, F., Rutland, C., Dittrich P., Raab A., Wirbelit F. (2000). Effects of Direct Water Injection on DI Diesel Engine Combustion, SAE J. Automot. Eng., 01-2938.

Durgun, O. (1991). A Practical Method for Calculation Engine Cycles, Union of Chambers of Turkish Eng. And Arc., Chamber of Mech. Eng., 383,18-29.

Durgun, O., Sahin, Z. (2009). Theoretical Investigation of Heat Balance in Direct Injection (DI) Diesel Engines for Neat Diesel Fuel and Gasoline Fumigation, Energy Conversion and Management, 50, 43-51.

Ferguson, R. (1986). Internal Combustion Engines-Applied Thermody, John Wiley & Sons, New York.

Hardenberg, H.O., Hase, F.W. (1979). An Empirical Formula for Computing the Pressure Rise Delay of a Fuel from its Cetane Number and from the Relevant Parameters of Direct Injection Diesel Engines, SAE Paper 790493.

Heywood, J.B. (1989). Internal Combustion Engines Fundamentals, McGraw Hill Book Company, New York.

Kızıltan, E. (1988). Effect of Alcohol Addition to Motor Fuels on Engine Performance, Master Thesis, KTU Graduate School of Natural and Applied Sciences, Trabzon, [in Turkish].

Kökkülünk, G., Gonca, G., Ayhan, V., Cesur, I., Parlak, A. (2013). Theoretical and Experimental Investigation of Diesel Engine with Steam Injection System on Performance and Emission Parameters, Applied Thermal Eng., 54, 161-170.

Ottikkutti, P., Gerpen, JV., Cui, KR. (1991). Multi-zone Modeling of a Fumigated Diesel Engine, SAE, 910076:1–21.

Pasternak, M., Mauss, F. (2009). Diesel Engine Cycle Simulation with a Reduced Set of Modeling Parameters Based on Detailed Kinetics, SAE, 01-0676.

Qi, K., Feng, L., Leng, X., Du, B., Long, W. (2011). Simulation of quasi-dimensional combustion model for predicting diesel engine perf., Appl. Math. Model., 35, 930-40.

Sahin, Z., Aksu, O. (2015). Experimental investigation of the effects of using low ratio n-butanol/diesel fuel blends on engine performance and exhaust emissions in a turbocharged DI diesel engine, Renewable Energy, 77, (279-290).

Sahin, Z., Durgun, O. (2007a). High speed direct injection (DI) light-fuel (gasoline) fumigated vehicle diesel engine, Fuel, 86:388–99. 597.

Sahin, Z., Durgun, O. (2007b). Theoretical investigation of effects of light fuel fumigation on Diesel engine performance and emissions, Energy Conversion & Management, 48, 1952–64.

Sahin, Z., Durgun, O. (2008). Multi-zone Combustion Modeling for the Prediction of Diesel Engine Cycles and Engine Perf. Par., Appl. Therm. Eng., 28, 2245-2256.

Sahin, Z., Tuti, M., Durgun, O. (2014). Experimental Investigation of the Effects of Water Adding to the Intake Air on the Engine Performance and Exhaust Emissions in a DI Automotive Diesel Engine, Fuel, 115:884-895.

Savioli, T. (2015). CFD Analysis of 2-Stroke Engines, Energy Procedia, 81, 723-31.
Shrivastava, R., Hessel, R., Reitz, R.D. (2002). CFD Optimization of DI Diesel Engine Performance and Emissions Using Variable Intake Valve Actuation with Boost Pressure, EGR and Multiple Injections, SAE, 2002-01-0959.

Sindhu, R., Amba Prasad Rao, G., Madhu Murthy, K. (2014). Thermodynamic Modelling of Diesel Engine Processes for Predicting Engine Performance, International Journal of Applied Engineering and Technology, Vol. 4 (2).

Tutak, W., Jamrozik, A. (2016). Validation and optimization of the thermal cycle for a diesel engine by computational fluid dynamics modeling, Appl. Math. Model., 40, 6293–6309.

Tuti, M. (2012). Experimental Investigation of the Effects of Water Adding to the Intake Air on Engine Performance and Exhaust Emissions in Diesel Engines, Master Thesis, KTU Institute of Science, Trabzon, Turkey [in Turkish].